

A Soft, Fast and Versatile Electrohydraulic Gripper with Capacitive Object Size Detection

Zachary Yoder, Daniela Macari, Gavriel Kleinwaks, Ingemar Schmidt, Eric Acome, and Christoph Keplinger*

Soft robotic grippers achieve increased versatility and reduced complexity through intelligence embodied in their flexible and conformal structures. The most widely used soft grippers are pneumatically driven; they are simple and effective but require bulky air compressors that limit their application space and external sensors or computationally expensive vision systems for pick verification. In this study, a multi-material architecture for self-sensing electrohydraulic bending actuators is presented that enables a new class of highly versatile and reconfigurable soft grippers that are electrically driven and feature capacitive pick verification and object size detection. These electrohydraulic grippers are fast (step input results in finger closure in 50 ms), draw low power (6.5 mW per finger to hold grasp), and can pick a wide variety of objects with simple binary electrical control. Integrated high-voltage driving electronics are presented that greatly increase the application space of the grippers and make them readily compatible with commercially available robotic arms.

generally designed for specific tasks and excel greatly in controlled and repetitive environments. They are typically made more versatile through the addition of external sensors, advanced controls, or computer vision.^[1] This results in systems that are not only complex and costly but also computationally expensive to operate.^[1,2] The field of soft robotics draws inspiration from nature to create systems that replace rigid links and DC motors with soft functional materials like muscle and skin, thereby simplifying controls via embodied intelligence.^[3]

Since Hirose et al. introduced a conformal gripper in 1978,^[4] a variety of soft robotic grippers have demonstrated the effectiveness of this new bio-inspired approach to robotics through their ability to grasp a wide variety of objects and carry out tasks that would be more complex

with traditional robotic systems^[5] (well summarized by Shintake et al.^[6] and Zaidi et al.^[7]).

Soft pneumatic grippers stand out due to their simple and versatile design, fast gripping speed, and effective grasping performance.^[5e] Their curling actuation principle coupled with a soft continuum structure makes these actuators well suited for gripping tasks and have led to a variety of highly adaptable systems,^[5c-e,g,8] as well as successful implementation in commercial manufacturing environments (Soft Robotics Inc., softroboticsinc.com). However, most pneumatic grippers require bulky, inefficient, and tethered air compressors and valve arrays, limiting their application space.^[6,7,9] Pneumatic grippers driven by untethered pumps have been shown, but suffer from slower actuation speeds.^[10] Embedded sensors have been used to provide grasp feedback^[11] but this approach adds complexity to the system.

In this work, we present a multi-material architecture for electrohydraulic bending actuators that are soft, fast and can simultaneously be used for actuation and sensing. These bending actuators enable versatile and reconfigurable grippers that are electrically driven and use capacitive self-sensing for pick verification and object size detection. We show that this class of electrohydraulic grippers are readily compatible with compact high-voltage driving electronics and can be easily integrated with commercially available robotic arms (**Figure 1**).

The electrohydraulic grippers build on HASEL (hydraulically amplified self-healing electrostatic) artificial muscles;^[12] we introduce a tunable fabrication procedure where


1. Introduction

Gripping is a fundamental mode of interaction with the environment. Robust, versatile, and adaptable robotic grippers that can operate in dynamic and unpredictable situations have long been sought after for various uses such as manufacturing, agriculture, and medical applications. Traditional rigid grippers are

Z. Yoder, D. Macari, I. Schmidt, C. Keplinger
Robotic Materials Department
Max Planck Institute for Intelligent Systems
Heisenbergstraße 3, 70569 Stuttgart, Germany
E-mail: ck@is.mpg.de

Z. Yoder, G. Kleinwaks, I. Schmidt, E. Acome, C. Keplinger
Paul M. Rady Department of Mechanical Engineering
University of Colorado, Boulder
1111 Engineering Drive, Boulder, CO 80309, USA

C. Keplinger
Materials Science and Engineering Program
University of Colorado, Boulder
1111 Engineering Drive, Boulder, CO 80309, USA

 The ORCID identification number(s) for the author(s) of this article can be found under <https://doi.org/10.1002/adfm.202209080>.

© 2022 The Authors. Advanced Functional Materials published by Wiley-VCH GmbH. This is an open access article under the terms of the Creative Commons Attribution License, which permits use, distribution and reproduction in any medium, provided the original work is properly cited.

DOI: 10.1002/adfm.202209080

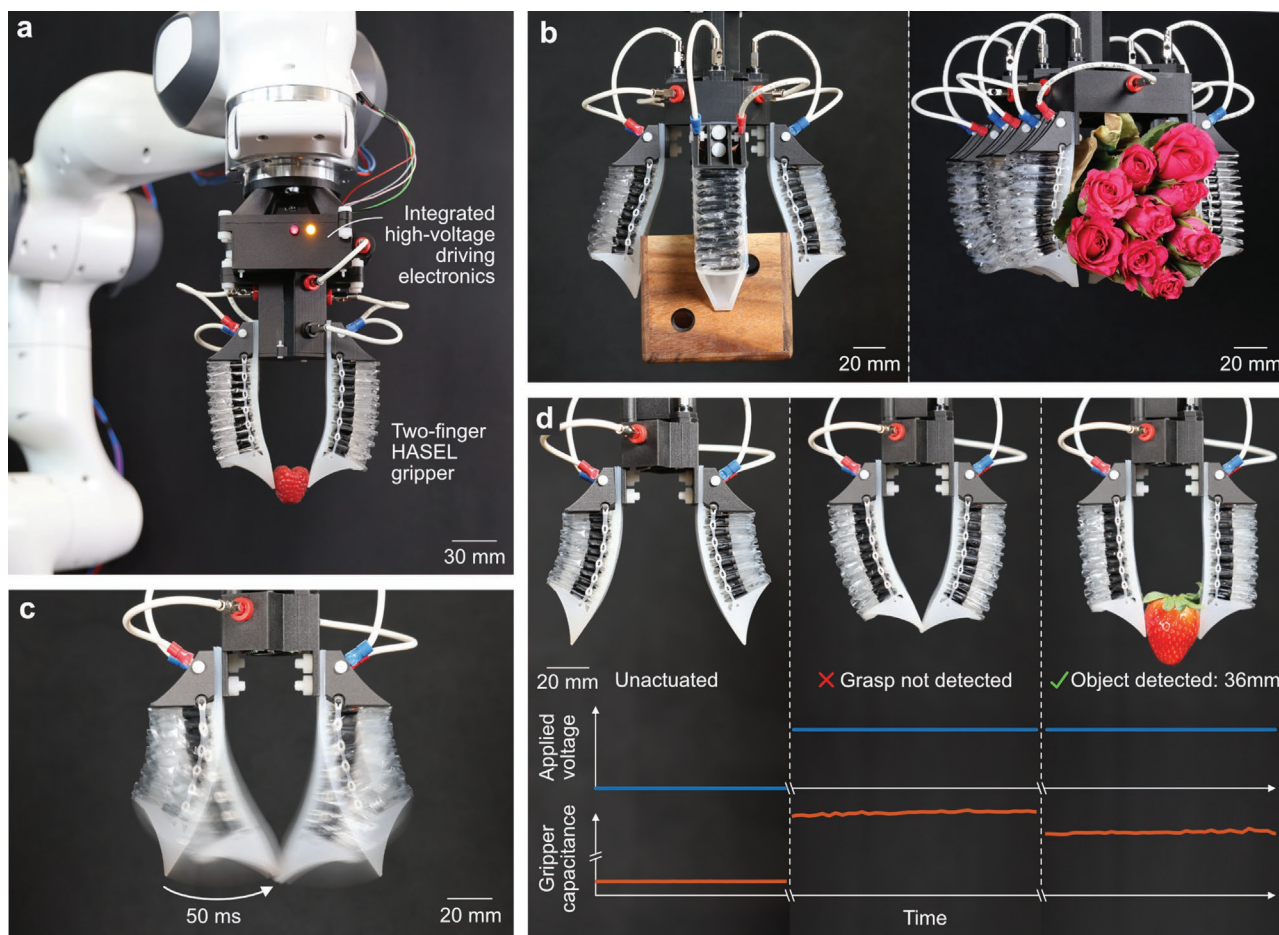


Figure 1. A soft, fast, and self-sensing electrohydraulic gripper. a) The gripper can be actuated by integrated high-voltage driving electronics, allowing for easy integration with a commercially available robotic arm. Its soft continuum structure allows for grasping of delicate objects without inflicting damage. b) The gripper is reconfigurable and can be oriented in many different ways, such as a four-finger or six-finger gripper. c) Fast, electrohydraulic actuation enables a single finger to reach 95% of its steady-state position in just 50 ms. d) The gripper features embedded self-sensing; each finger can simultaneously be used as an actuator and a sensor. This allows for real-time pick verification and object size estimation.

folded HASEL actuators are precisely aligned via acrylic combs and constrained on one side by a silicone-based strain-limiting layer. This design and fabrication approach results in multi-material actuators that feature adjustable bending radii governed by actuator spacing and allows for versatile optimization for various robotics applications.

Soft grippers based on HASEL actuators have previously been presented^[12a,c,13] but none have achieved versatile, robust and tunable gripping with fully soft continuum actuators in a practical and reconfigurable package. Likewise, no electrohydraulic gripper has utilized capacitive self-sensing for grasp feedback and object size detection.

In this work, we characterize the individual bending actuator, or “finger,” and show controllable pinch force up to 0.7 N, repeatable change in capacitance with respect to displacement, and fast, tunable grip speeds (as little as 50 ms to grip). The actuation of each finger can be easily controlled by varying the applied voltage (Movie S1, Supporting Information). We show various gripper configurations that can grasp a wide variety of objects, including delicate fruits, only using binary electrical control and we characterize grip performance with pull-off tests (pull-off

forces up to 2.7 N). Additionally, we present an algorithm that uses the capacitive self-sensing properties of HASEL actuators to accomplish two industrially relevant tasks: the gripper can electrically detect if an object was successfully grasped, and it can estimate the size of the grasped object (Figure 1d).

Finally, we leverage recent advances in the field of miniature high-voltage electronics^[14] to design low-profile driving electronics that integrate with the gripper’s central mount, thus eliminating the need for bulky high-voltage amplifiers and making the gripper readily compatible with commercially available robotic arms.

2. Results

2.1. Actuation Principle

Each multi-material bending actuator contains multiple HASEL pouches consisting of a thermoplastic shell (15 μm mylar film, PetroPlast) filled with liquid dielectric (5 cSt silicone oil, Roth). Electrodes that cover half of the pouch are printed on both sides

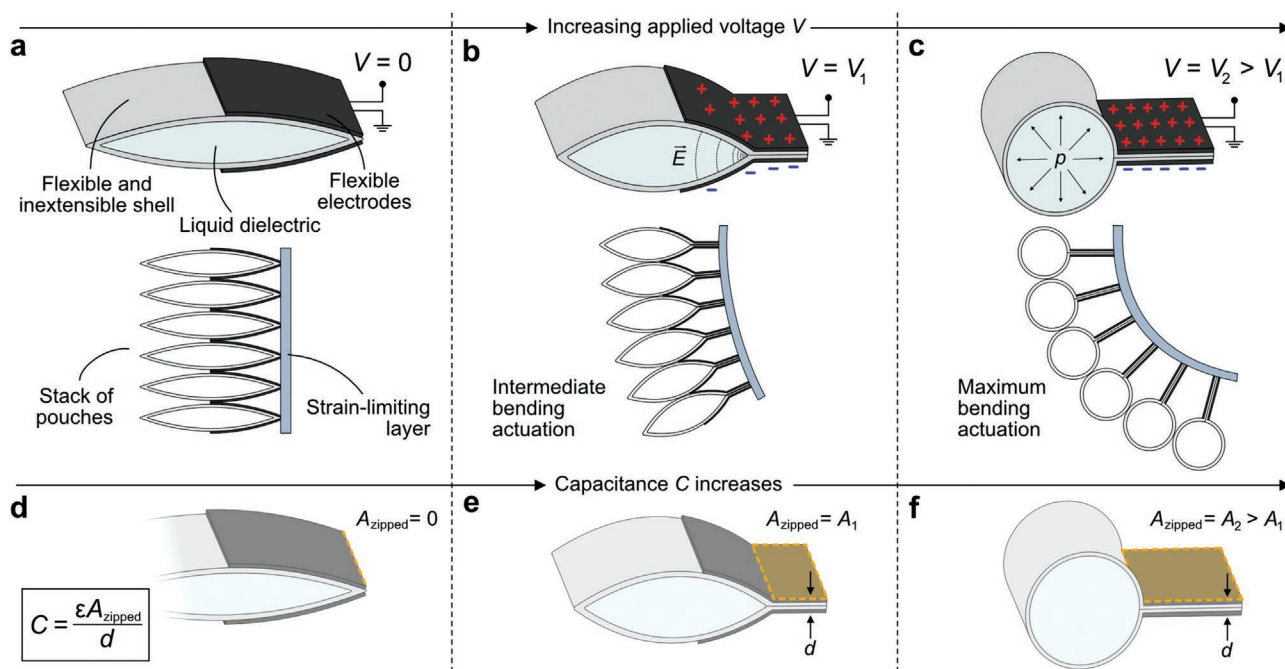


Figure 2. Multi-material architecture for a self-sensing electrohydraulic bending actuator. a) An individual HASEL (hydraulically amplified self-healing electrostatic) actuator is made up of a flexible but inextensible shell that is filled with liquid dielectric and has flexible electrodes on both sides covering half of the pouch. A stack of these actuators, constrained on one side with a strain-limiting layer, comprises a multi-material bending actuator. b) Applying high voltage to the electrodes creates an electric field that causes them to zip together and drives shape change of the pouch. One side of the stack expands while the other does not, resulting in bending actuation. c) With increasing voltage, the hydraulic pressure in the pouch increases until maximum bending actuation is reached. d–f) Actuation strain is proportional to the zipped area of the electrodes and consequently to capacitance. Monitoring the capacitance therefore enables self-sensing feedback about the deformation state of the actuator.

using conductive carbon ink (CI-2051, EMS Adhesives). Under applied high voltage, Maxwell stress causes the electrodes to zip together, thereby displacing the fluid in the pouch, increasing the hydraulic pressure in the non-electrode region and driving shape change (Figure 2a–c).^[12a,b]

To turn a single, expanding pouch into a larger continuum-bending actuator we stack multiple HASEL pouches together, such that application of high voltage results in uniform actuation of all of the pouches. We cure a soft but inextensible polymer layer onto the electrode side of the stack. Under applied high voltage, the side of the pouches that are not covered by electrodes expands while the strain-limited-side of the finger remains the same length, resulting in the overall bending of the continuum structure (Figure 2a–c).

As voltage increases, and actuation consequently progresses, the zipped area of the electrodes gets larger, resulting in an increase in capacitance that is related to the displacement of the actuator (Figure 2d–f).^[15] Various techniques exist to measure the capacitance of electrostatic actuators in real-time^[5i,16] allowing for this multi-material bending structure to be simultaneously used as an actuator and a sensor.

2.2. Fabrication of Multi-Material Electrohydraulic Bending Actuators

To realize the proposed bending actuators, we heat-seal a series of pouches, screen-print electrodes, and fill each pouch with a

liquid dielectric, following the technique described by Mitchell et al.^[12c] (Figure 3a,b).

We fold the series of pouches back and forth onto itself (Figure 3c) and use a comb-like acrylic fixture to hold the resulting stack of pouches in an uncured silicone bath. Separately, we fabricate ancillary components (Figure 3d) and add the fingertip and plastic separators to the bath (Figure 3e). After allowing the silicone to cure, we remove the “finger” and add a 3D-printed mount and the elastic band for restoring force, completing the fabrication process (described in detail in the Supporting Information).

2.3. Actuation Performance of Single Fingers

We characterized the grip force, capacitive self-sensing behavior, speed and energy consumption of a representative finger, shown in Figure 4.

A dual-mode muscle lever (310-LR, Aurora Scientific) with a custom 3D-printed lever arm (Onyx filament, Markforged Onyx One) stepped through evenly-spaced points along the actuation path of the fingertip. At each point, the gripper was actuated four times and the fingertip was pressed against the muscle lever arm. The force was measured by the muscle lever and the capacitance was measured using AC signal analysis (further described in Materials and Methods). Both were averaged over the 4 cycles (Figure 4b,c). Each curve in Figure 4b,c represents a different actuation voltage (4–7 kV). A video of

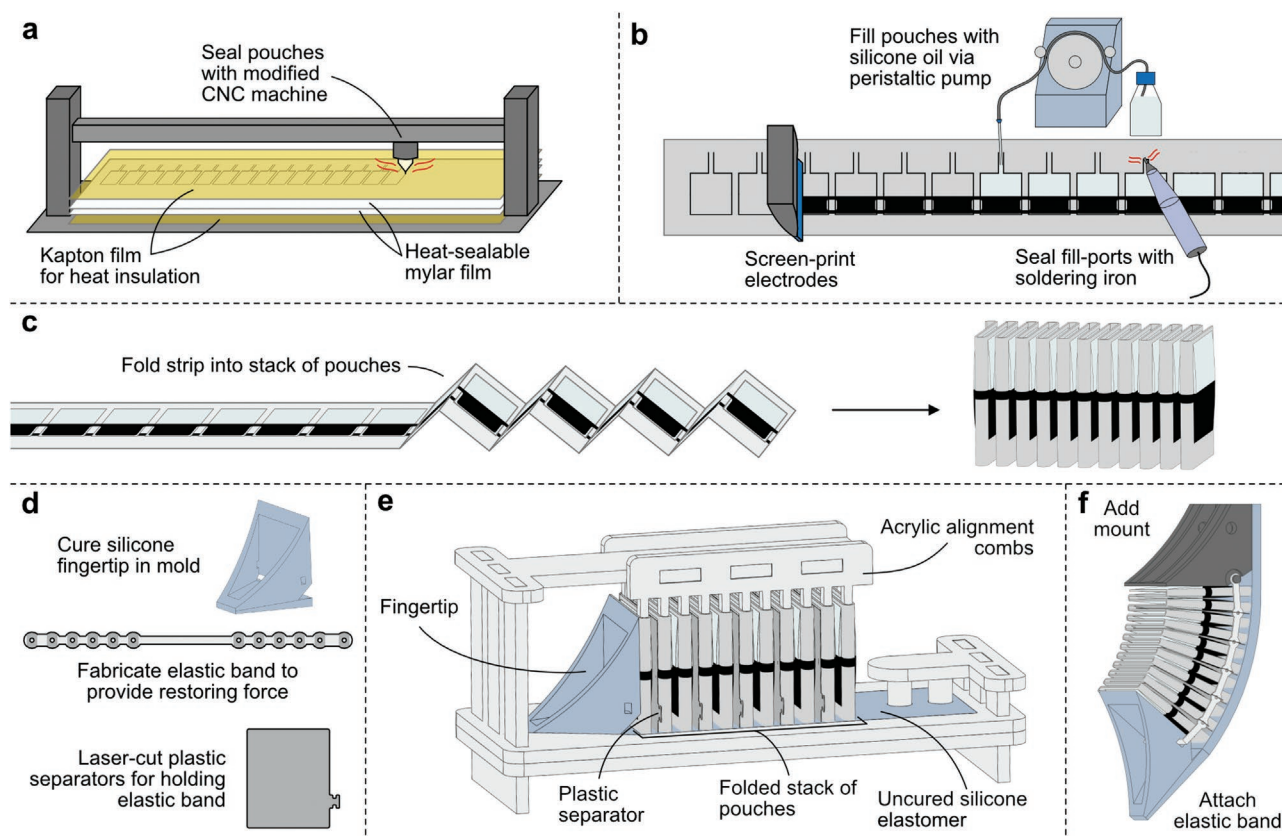


Figure 3. Fabrication steps for a single multi-material bending actuator, called a “finger.” a) 2 layers of mylar film are heat-sealed together into a strip of 22 individual pouches with open fill-ports. b) Electrodes are screen printed onto both sides of the strip of pouches, the pouches are filled with silicone oil, and the fill ports are sealed with a soldering iron. This results in a strip of 22 HASEL actuators connected in series. c) The strip of pouches is folded into a continuum stack. d) In parallel, a silicone fingertip, an elastic band and plastic separators are fabricated. e) Custom acrylic combs are used to hold the stack in place and plastic separators are added between folds. The entire structure is placed into a bath of uncured silicone elastomer along with the fingertip and left to cure at room temperature. f) The acrylic alignment combs are removed, a 3D-printed mount is added and the elastic bands are attached.

the test can be seen in Movie S2 (Supporting Information). The gripper applied forces up to 0.7 N throughout a range of ≈ 58 mm (Figure 4b) and the force decreased with lower voltage and higher stroke. The capacitance of the finger increased with higher stroke, but plateaued close to its maximum stroke.

To analyze the performance of the gripper over time, we repeated the test shown in Figure 4a at a fixed displacement (roughly halfway through the actuation range of the finger). We cycled a new finger at 6 kV and measured the tip force and capacitance (Figure S3, Supporting Information). The results show that the force and capacitance initially increase but plateau after ≈ 500 cycles, indicating the existence of an initial stabilization period (the data shown in Figure 4b,c was taken after ≈ 640 cycles thus reflecting the long-term performance of the gripper). The finger broke down electrically at 2650 gripping cycles. Individual HASEL actuators can achieve millions of cycles;^[12a] the gripper shown here is a rather complex device built from dozens of individual actuators that are manually fabricated and assembled, leading to many potential points of failure due to the introduction of defects. The specific gripper tested here broke down through a heat-sealing line indicating that more precise fabrication techniques could mitigate this type of failure.

We analyzed the speed and power consumption of the finger when actuated with a square wave voltage signal (Figure 4d). The finger demonstrated fast actuation speeds – as little as 50 ms to reach 95% of its steady-state position (Figure 4e). It overshoot its steady-state position during actuation and relaxation; Figure 4e shows the tunability of the finger by presenting two approaches to reducing this overshoot.

First, HASEL actuators can be filled with a variety of liquid dielectrics, including high-viscosity fluids that can lead to increased damping of the actuator.^[17] In one finger, we filled the individual pouches with 500 cSt silicone oil (Roth), rather than the 5 cSt silicone oil (Roth). This approach increased the damping ratio ζ of the finger from 0.29 (5 cSt) to 0.47 (500 cSt), leading to a substantial decrease in the overshoot of the fingertip position but resulting in a much longer relaxation time. To calculate the damping ratio, as well as other relevant dynamic parameters, we idealized each finger as a mass-spring-damper system and show the resulting values in Table S1 (Supporting Information).

Our second approach was to actuate the nominal finger (5 cSt silicone oil) with a square wave that was modified for open-loop damping in an attempt to maintain a fast

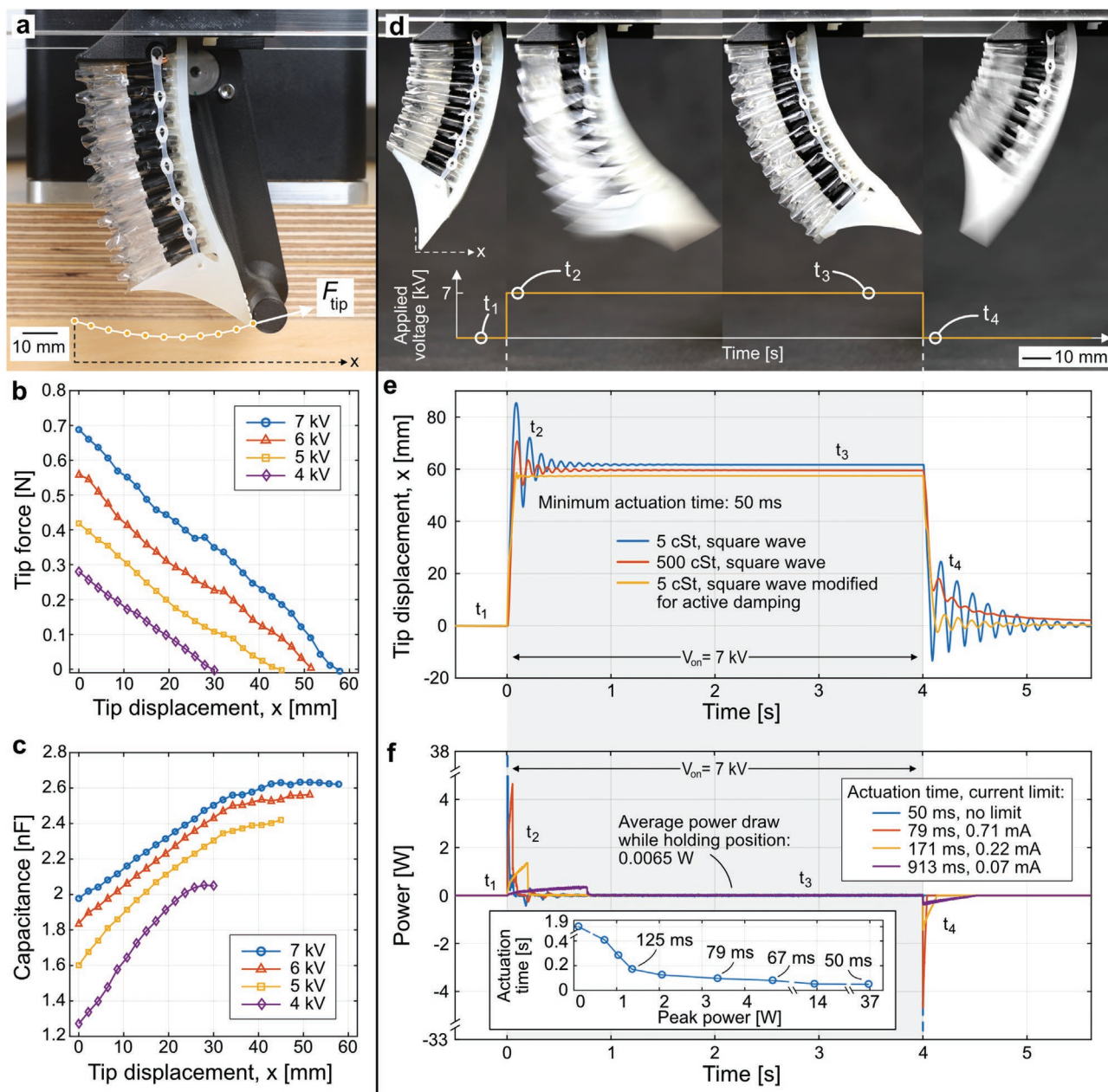


Figure 4. Characterization of actuation performance of a single finger. a–c) The fingertip force and capacitance of the finger was measured at various displacements within the finger’s actuation range. With greater displacement the fingertip force decreased while the capacitance increased; the capacitance eventually reached a plateau at high displacements. d) The response of a single finger to a square-wave actuation signal demonstrated fast and tunable actuation. e) The finger reached 95% of its steady-state position in as little as 50 ms. The overshoot was reduced by using higher viscosity liquid dielectric as well as by actuating the finger with a custom voltage signal. f) Due to its electrostatic catch-state, the finger required only 6.5 mW to hold its position in the actuated (grasping) state. The fastest actuation speeds required high spikes of power, but the finger still actuated rapidly under lower power constraints (inset).

response while reducing overshoot. The signal consisted of a voltage pulse superimposed on the actuation and relaxation parts of the square-wave cycle, and is further described in Figure S4 (Supporting Information). This substantially reduced the overshoot during both actuation and relaxation, but added complexity to the overall actuation scheme and required robust amplifying electronics. Both damping strategies resulted in smaller maximum fingertip displacement,

and a comparison video is shown in Movie S3 (Supporting Information).

We measured the power consumption of the nominal finger (5 cSt silicone oil) by recording the voltage drop over a shunt resistor. First, the finger drew an initial power spike for actuation, then an average of only 6.5 mW to hold its actuated position (Figure 4f). The low power draw to hold its state was due to the inherent electrostatic catch-state native to HASEL actuators,

further described by Acome et al., Kellaris et al., and Yoder et al.^[12a,13a,d] The actuation scheme based on active voltage damping resulted in a secondary power spike (Figure S5, Supporting Information). A peak power of 37 W was required for the fastest actuation speed. To simulate actuation with lower-power mobile electronics, we also analyzed the power consumption and speed of the finger under power-limited conditions by limiting the current output of the high-voltage amplifier (TREK 610E, 5012) to a range of values (0.04 to 12 mA) (Figure 4f; inset, Figure S6, Supporting Information). Slower actuation speeds drew substantially less peak power (<5 W peak power for an actuation time of 79 ms, for example).

2.4. Performance of Multi-Finger Soft Grippers

In this work, we show versatile two-, four-, and six-finger grippers, each of which allowed for damage-free gripping of a multitude of objects with only on/off voltage control (Figure 5a–c).

Within each mount, the fingers were connected electrically to a common driving channel, therefore one high-voltage input controlled all connected fingers. The gripper deformed around objects and gripped using the conformal strain-limiting layer on the inside of the finger, and carried out nimble and gentle pinching grasps with its fingertip.

We characterized the strength of the two- and four-finger grippers with a pull-off test designed to measure the maximum force required to pull an object out of grasp and thus mimic practical gripping scenarios. We 3D-printed spheres ranging in size from 20 to 80 mm (generic PLA, Prusa i3 mk3s) and attached them with a string to a dual-arm muscle lever (310C-LR, Aurora Scientific) that applied a linearly increasing force ramp until the object was pulled out of grasp (Figure 5d; Movie S4, Supporting Information). We repeated the test four times for each object.

While the results of this test depend on the geometry and surface characteristics of the grasped object, we used the pull-off test to provide an intuitive overview of the practical grasping capabilities of the specific gripper design introduced here and to contextualize its performance with other work.

Figure 5e shows the results of this test indicating that the pull-off force increases with increasing numbers of fingers and decreasing finger spacing. Wider finger spacing allowed for a larger workspace, and narrower spacing allowed for higher pull-off forces, as well as for picking smaller objects. In both two-finger configurations shown, the fingers contacted each other upon actuation when there was no object in between – in theory allowing for arbitrarily small objects to be grasped. The smallest object that we tested was the slim ID card shown in Figure 5a (0.8 mm thick), but precisely picking smaller objects can be improved by changing the fingertip design and the overall size of the fingers.

When considering just the mass of the fingers, the pull-off test resulted in an object mass to gripper mass ratio of 1.5–1.7 (two- and four-finger grippers, respectively); this ratio is compared for many soft robotic gripping technologies in Shintake et al.^[6] Future materials for HASEL actuators are predicted to feature substantially higher energy density and would thereby enable higher-force grippers.^[18]

2.5. Robustness of the Gripper

The gripper is robust to conditions outside of the normal vertical gripping mode and can be used in a variety of orientations (Figure 6a,b). In Figure 6a, the silicone layer in each finger provided sufficient stiffness to support the weight of the finger and the object in grasp, while in Figure 6b the silicone band supported the weight of the finger against gravity.

During testing, we inadvertently drove the grippers into contact with target objects. Due to the entire soft continuum structure of the fingers, these collisions resulted in no harm to the fingers, gripper assembly or supporting structures (Figure 6c–e; Movie S9, Supporting Information).

2.6. Capacitive Self-Sensing for Pick Verification and Object Size Detection

As shown in Figure 2d–f and Figure 4c, the capacitance of each finger varied with the degree of actuation. We designed a sensing scheme and feedback algorithm, shown in Figure 7, which used the relationship between capacitance and displacement to detect if a grasp was successful, and to estimate the size of the grasped object.

To measure the capacitance of each finger, we used the capacitive sensing technique introduced by Keplinger et al.^[16c] in an experimental setup that included a MATLAB program (R2020a), a data acquisition device (USB-6212, National Instruments) and a high-voltage amplifier (TREK 610E). We superimposed a high-frequency, low-voltage AC sensing signal onto the low-frequency, high-voltage DC actuation signal and measured the response in the current of each finger independently via shunt resistors (Figure 7a). We then calculated the phase angle between the applied voltage and responding currents, from which the capacitance of each finger could be independently calculated (described in detail in Experimental Section).

We completed one calibration process per finger to create a lookup table $d(C)$ that returned fingertip displacement as a function of capacitance (Figure 7b). This lookup table was also used to create a critical capacitance value C_{crit} for each finger, where the relationship between capacitance and displacement was no longer one-to-one, which we refer to as the “grasp detection threshold.”

We then used the lookup table and grasp detection threshold as inputs to an algorithm which refreshed at 10 Hz (Figure 7c) while the gripper was actuated to maximum voltage (6 kV). The capacitance of each finger was calculated and compared to the grasp detection threshold. If the capacitance was greater than the threshold value, this indicated an unsuccessful grasp, while a capacitance less than the threshold value indicated a successful grasp. When a successful grasp was indicated, the displacement was looked up in $d(C)$ and added to the initial spacing of the fingers on the mount to arrive at an estimate of the size of the object.

We characterized the effectiveness of the size detection algorithm by measuring fruits and vegetables of different shapes and sizes, the results of which are shown in Figure 7d,e. We measured each object over six grasping cycles, with each grip lasting 4 s. The size detection effectively estimated the diameter of the

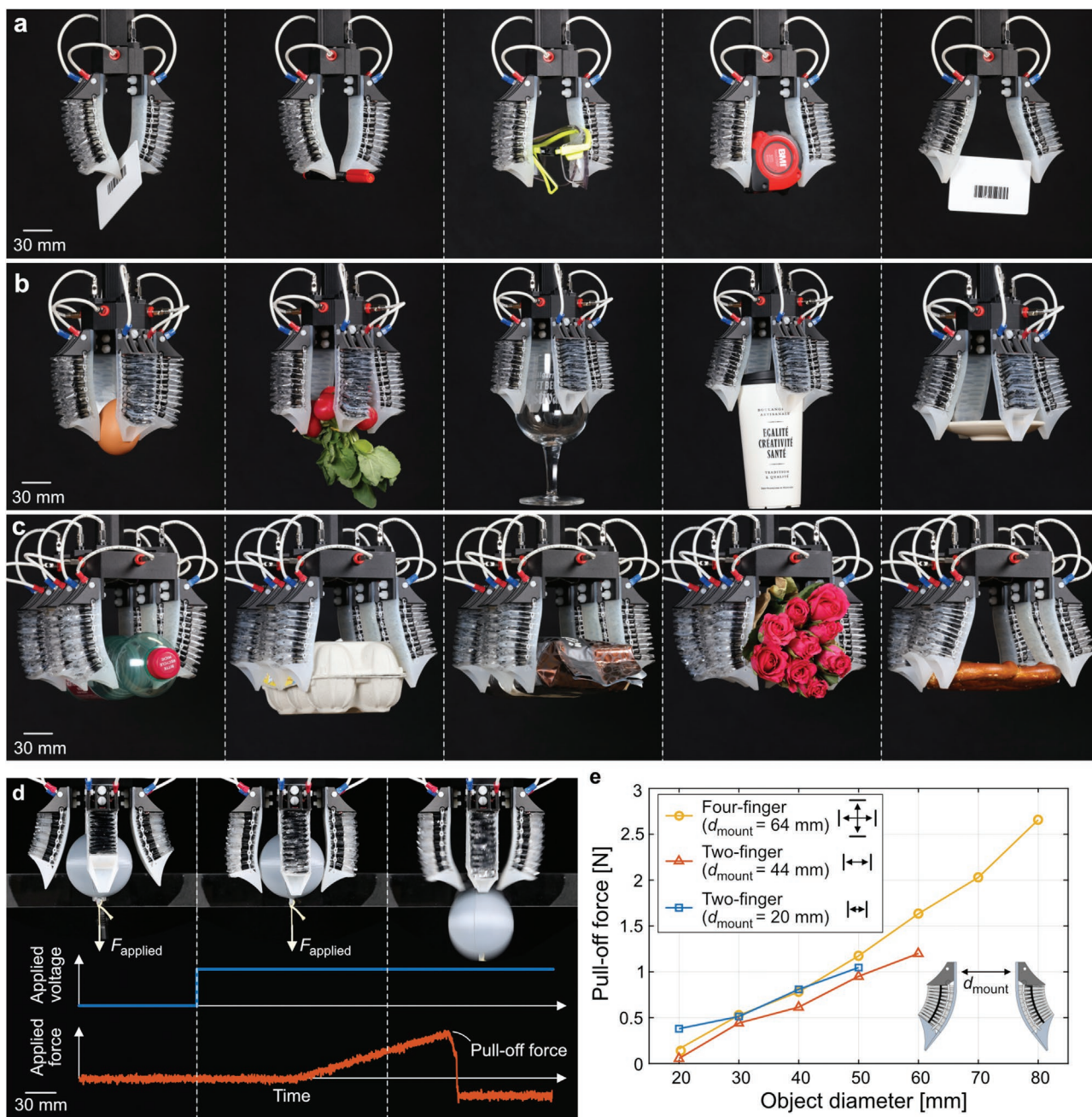


Figure 5. Versatility and reconfigurability of the soft gripper. The soft and conformal nature of the gripper enabled grasping of objects with various sizes, surfaces and form factors, including delicate, deformable, and irregularly shaped objects. a) A two-finger gripper grasping an ID card (slim), a pen, lab goggles, a tape measure and an ID card (wide). b) A four-finger gripper grasping an egg, a bundle of radishes, a beer glass, a coffee cup, and an espresso dish. c) A six-finger gripper grasping a plastic bottle, an empty egg carton, a bag of espresso beans, a flower bouquet, and a pretzel. d,e) The maximum force necessary to pull an object out of grasp was measured. Narrow finger spacing resulted in higher pull-off forces but reduced the workspace of the gripper.

object in grasp and had a maximum error of 3 mm when averaged over six cycles. The largest variability occurred with the smallest object (broccoli). During one of the cycles, an irregular grasp caused one finger to actuate much further than the other. The broccoli was successfully grasped, but the capacitance of the further-actuated finger crossed the grasp detection threshold and predicted an unsuccessful grasp. Thus, the object

size was calculated based only on the displacement of the other finger, resulting in a much lower size estimate.

To demonstrate the practical usefulness of the real-time grasp and size detection, we attached the gripper to a commercially available robotic arm (Panda, Franka Emika) and carried out two demonstrations. First, we demonstrated real-time grasp detection – the gripper was unable to lift a heavy weight and

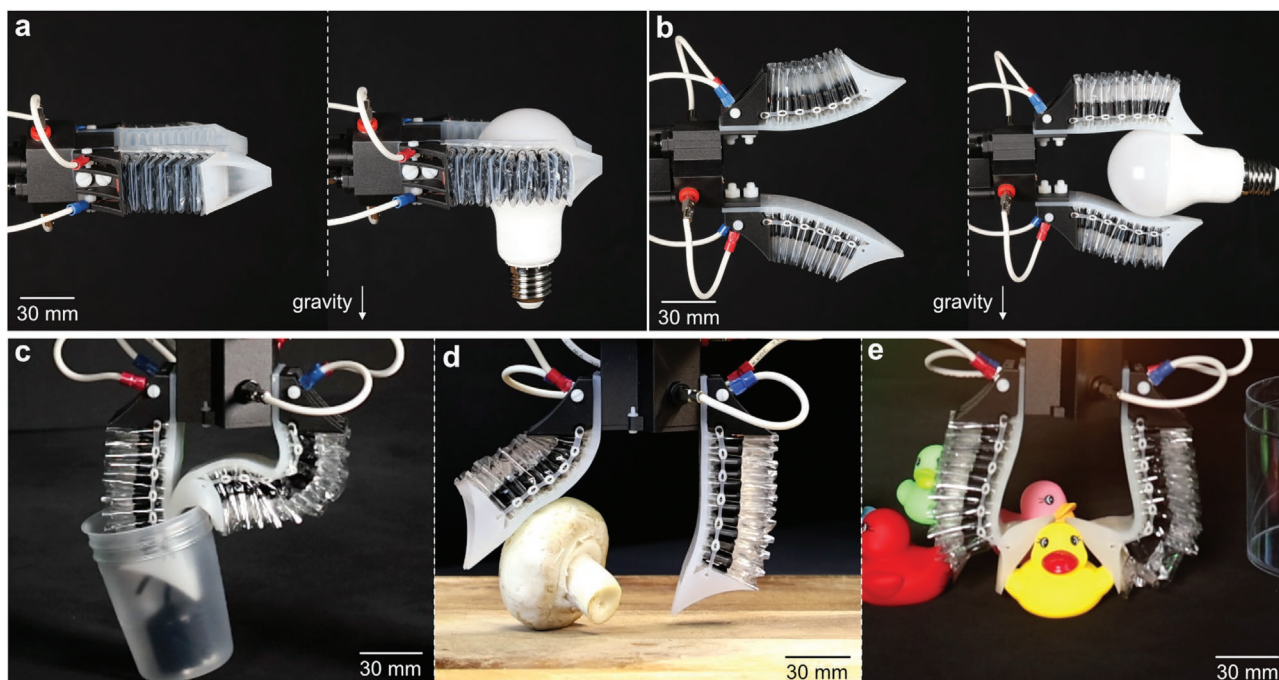


Figure 6. Robustness of the gripper. a,b) The gripper is mechanically robust and can be used in horizontal orientations. c–e) Its fully soft and conformal body prevents damage in case of inadvertent collisions.

indicated an unsuccessful grasp, but indicated a successful grasp when it picked up a lighter weight (Movie S5, Supporting Information). Second, we showed real-time size detection of some of the fruits and vegetables shown in Figure 7d (Movie S6, Supporting Information). Finally, we showed real-time size detection of a variety of tomatoes while the robotic arm followed a preprogrammed sorting routine to place the tomatoes into different buckets based on their size (Movie S7, Supporting Information).

2.7. Integrated High-Voltage Driving Electronics

For the experiments shown thus far, we used a bench-top high-voltage amplifier (TREK 610E) for actuation and sensing. To further increase the application space of the gripper, we designed compact high-voltage driving electronics that can readily interface with a standard robotic arm and with the gripper's central mount (Figure 8).

This electronics package, based on work by Mitchell et al.,^[14a] eliminated the need for a benchtop high-voltage amplifier for actuation, but did not include capacitive sensing capabilities. Additionally, it could not provide a high enough slew rate to implement the voltage-damping actuation scheme (Figure 4e; Figures S4 and S5, Supporting Information).

The main components of the electronics package included a 5 W high-voltage amplifier (5VV10, Pico Electronics) and an H-bridge orientation of custom optocouplers (OC100SG, Voltage Multipliers Incorporated), both of which were controlled by a custom microcontroller (Figure 8b). The circuit schematic and bill of materials are shown in Figure S7 and Table S2 (Supporting Information) respectively. We used the

H-bridge orientation to reverse the polarity of the high voltage in order to minimize the accumulation of space charges, a phenomenon seen in many electrostatic actuators which decrease their strain over repeated, single-polarity high-voltage DC cycles.^[12d]

All necessary high-voltage driving electronics were contained within this package and fit inside a 75 mm x 75 mm x 29 mm box – the only external connections needed were 5 V/ 1 A power, serial communication wires and a high-voltage kill switch. The high-voltage output was monitored via a voltage divider which allowed us to implement a PID controller and enabled faster actuator charging and thus higher actuation speeds. For the two-finger gripper, we achieved a maximum actuation speed of 300 ms (Figure S8, Supporting Information).

This package is compatible with commercially available robotic devices, such as a robotic arm (Panda, Franka-Emika), and can be used to carry out practical tasks. In Figure 8c and Movie S8 (Supporting Information), we used the fast actuation speed of the gripper to rapidly tidy up toys. Each toy was in a different orientation, but no additional controls were required to quickly grasp each object.

3. Discussion and Conclusion

The multi-material soft grippers presented in this work are based on an active continuum structure that utilizes electrohydraulic actuation to achieve fast, electrically-controlled gripping with capacitive self-sensing feedback, providing many key benefits over existing soft grippers (Tables S3 and S4, Supporting Information). The combined actuation and sensing scheme as well as the grasp feedback algorithm presented here are

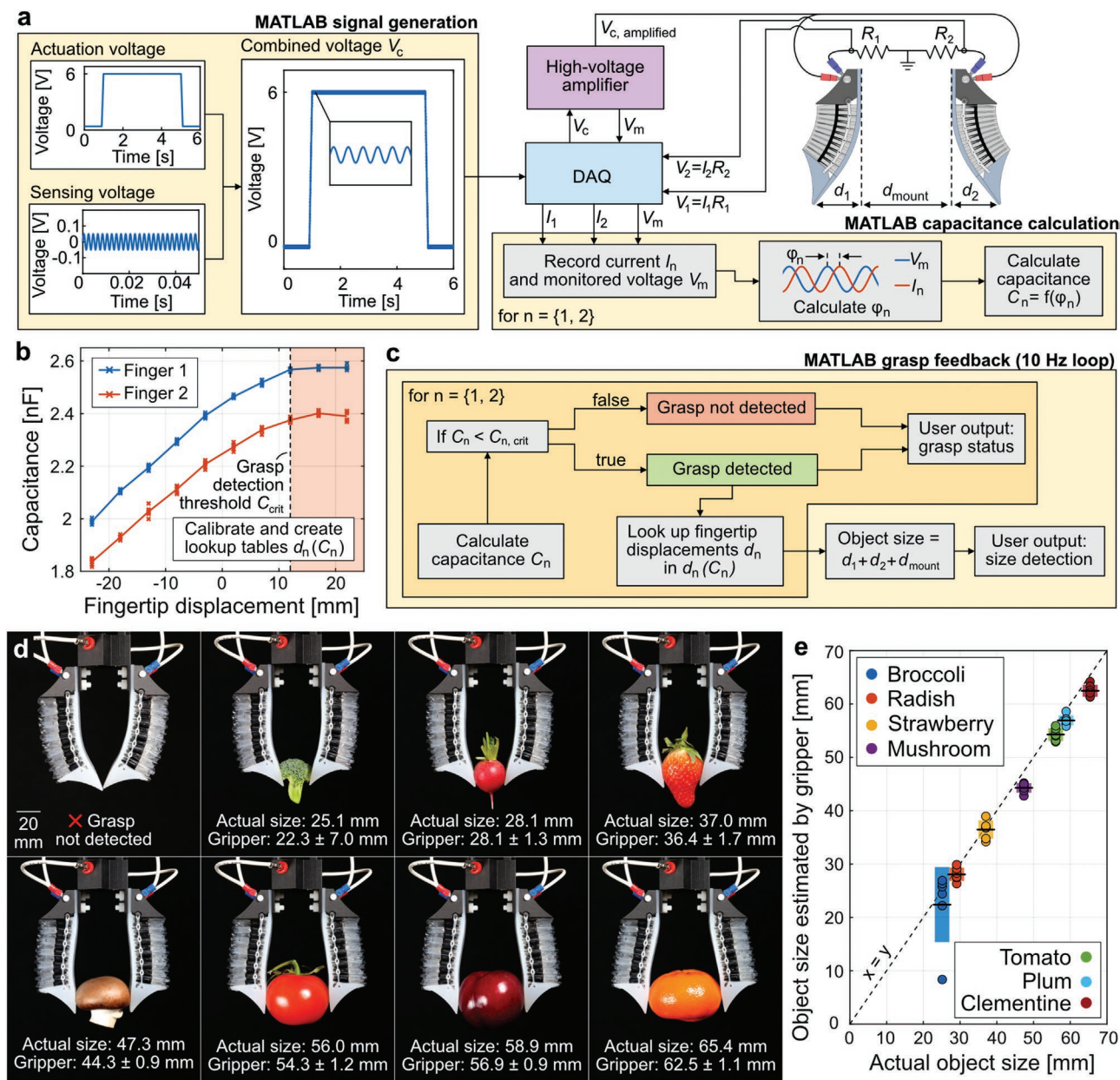


Figure 7. Real-time pick verification and object size estimation based on capacitive self-sensing. a) Method to calculate the capacitance of each finger using a low-voltage sensing signal superimposed onto the high-voltage actuation signal. b) Each finger was calibrated one time to map the relationship between capacitance and fingertip displacement. Near the maximum stroke of each finger the capacitance plateaued and a “grasp detection threshold” was set at this value. c) Following the presented algorithm, the capacitive self-sensing of the gripper was used to detect successful grasp and estimate object size in real time. d,e) The grasp and size detection worked effectively for objects of various sizes.

relatively simple yet highly effective, opening a variety of new research paths in robotics.

3.1. Electrohydraulic Actuation with Self-Sensing

In this work, we only characterized the relationship between capacitance and displacement for gripping at the fingertip and we did not expand the relationship beyond this gripping mode. Additionally, the relationship between capacitance and displacement breaks down around maximum stroke, limiting

the effective self-sensing range. Future work could include machine learning techniques or more sophisticated capacitive sensing approaches to provide paths toward more complex actuation and detection modes.

3.2. Versatile Design

The multi-material architecture presented enables a wide variety of electrically-driven bending actuators with highly tunable actuation responses. The material, size, and spacing of

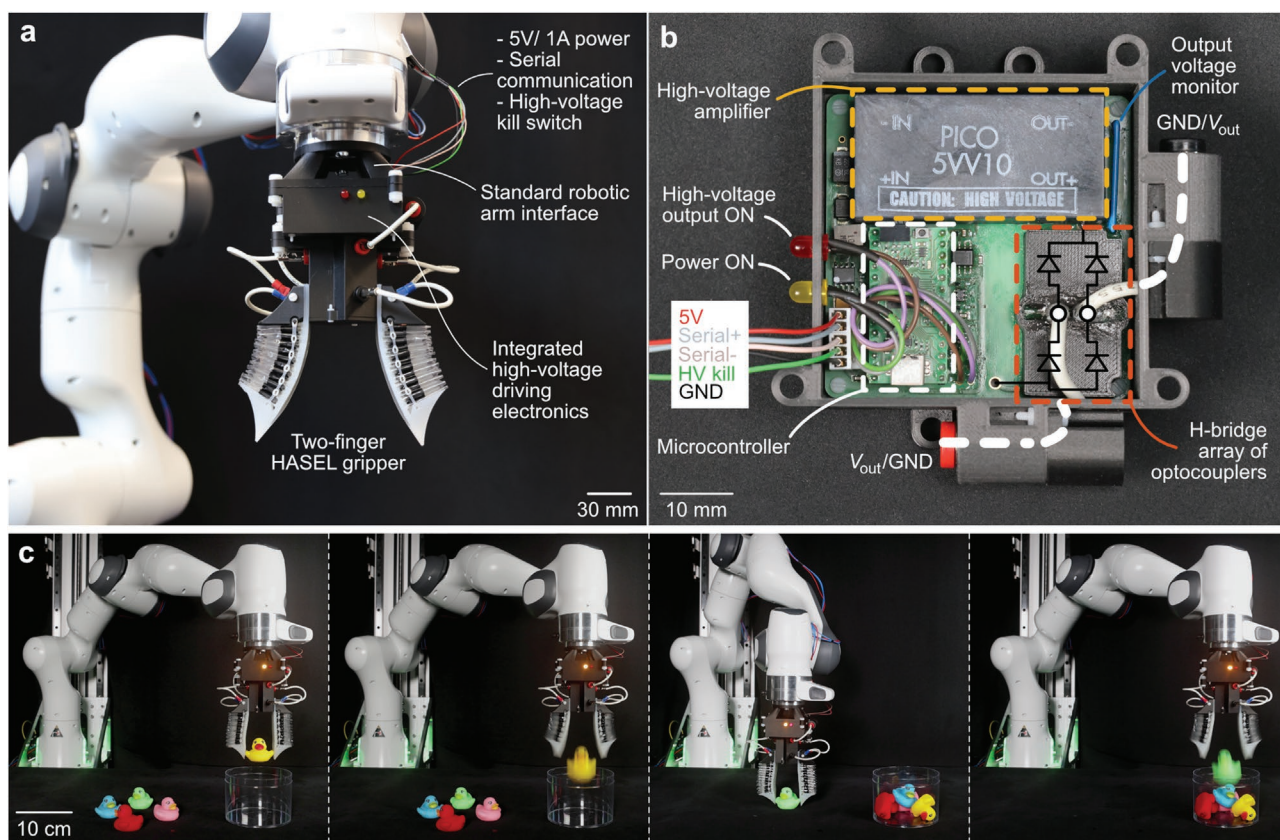


Figure 8. Using integrated high-voltage driving electronics, the gripper is readily compatible with commercial robotic arms. a) The entire gripper system weighs only 340 grams and contains all necessary electronics for high-voltage amplification and control. The driving electronics are connected to a 5 V / 1 A electrical input, serial communication via USB, and a high-voltage kill switch. b) A high-voltage amplifier (5 W) interfaces with an H-bridge of optocouplers and a microcontroller to enable controlled actuation and reversing polarity. c) The system was attached to a commercially available robotic arm and quickly tidied up toys (Movie S8, Supporting Information).

individual pouches, the makeup of the strain limiting layer, and the surface morphology of the gripping surface are all parameters that could immediately be tuned to achieve various performance metrics or to optimize these bending actuators for different robotics applications.

For example, applications requiring higher output forces could be made possible primarily by changing the performance of the individual pouches, which directly influences the overall performance of the multi-material bending actuator. Kellaris et al. reported that increasing the permittivity of the shell, the width of the electrodes and the applied voltage will result in higher output forces in Peano-HASEL actuators.^[18] However, higher permittivity films are not yet readily available for robotics applications, and increasing the width of the electrode will result in a bulkier bending actuator, thus we focused on demonstrating the scaling of the force with voltage for one prototypical geometry (Figure 4b).

The material used for the strain-limiting layer also offers wide design freedom, as many soft materials could be used so long as they satisfy the necessary requirements such as low bending stiffness, sufficient tensile strength, and soft and conformal surface.^[19]

The manual fabrication process and multi-component design represent drawbacks, especially when compared to

soft pneumatic grippers that can be molded or 3D-printed.^[20] While some steps of our manufacturing process could be simplified by using industrial electrode-printing or folding machines, the elastic band that provides restoring force is a component that involves tedious manufacturing and is prone to failure. In the future a new, robust strategy to provide restoring force should be developed to enable industrial use.

3.3. Integrated High-Voltage Driving Electronics

The integrated high-voltage electronics package contains all necessary components for gripper actuation and is made from commercially available components. This eliminates the need for bench-top high-voltage amplifiers for actuation and offers a concrete path for untethered operation in commonly proposed soft robotics use cases such as agriculture, disaster response, or space exploration.

The electronics package presented actuated a two-finger gripper in 300 ms which is relatively slow compared to 50 ms when actuated with the bench-top amplifier. Higher-power compact amplifiers are commercially available and could allow for the highest actuation speeds, even in multi-finger gripper

configurations that have higher capacitive loads (Ultravolt series, Advanced Energy, for example).^[14a]

The integrated electronics package presented is not immediately compatible with our self-sensing method; the real-time capacitive sensing was carried out using a benchtop high-voltage amplifier (TREK 610E). Ly et al. presented miniaturized capacitive self-sensing circuitry that could be integrated into the system^[15] and Tairyeh et al. presented a technique for multi-actuator sensing on a single physical channel, illustrating paths for future research in this area.^[21]

Tradeoffs between safe current limits and fast actuation speeds must be considered when designing electrohydraulic actuators and corresponding high-voltage driving electronics. The exposed electrodes of the actuators could result in electrical discharge through a human operator^[22] and electrical breakdown or corona discharge could serve as an ignition source. Various techniques exist to mitigate these risks, including encapsulating the actuators or limiting their maximum capacitive discharge (discussed further in Rothmund et al.^[12d]).

Overall, the multi-material architecture for self-sensing electrohydraulic bending actuators introduced here provides unique, new capabilities beyond traditional grippers and further advances the state of the art of soft grippers thereby offering new solutions in fields such as agriculture, manufacturing and disaster response while opening up new avenues of research in materials innovation, robotic systems design, sensing, and machine learning.

4. Experimental Section

Technique for Capacitive Self-Sensing: To calculate the capacitance of each finger, we idealized each finger as an RC circuit, with constant resistance R (resistance of the electrodes), and variable capacitance C (due to the charges stored by the electrodes). We superimposed a 1000 Hz, 50 V AC voltage signal onto the high-voltage DC signal and used this combined signal to actuate the finger (the AC signal was small enough that it did not noticeably affect actuation). We calculated the current by measuring the voltage drop over a shunt resistor on the ground side of each finger.

The overall impedance of the actuator Z is described in Equation 1

$$Z = \frac{V_s}{I} \quad (1)$$

where V_s is the magnitude of the applied AC voltage and I is the magnitude of the measured current. Due to the capacitance of the system, the measured current was out of phase with the applied voltage by the phase angle φ . MATLAB was used to calculate φ and to subsequently calculate the capacitive reactance X_c using Equation 2.

$$X_c = Z \sin(\varphi) \quad (2)$$

The capacitance C can be found using Equation 3 from the capacitive reactance X_c and the frequency of the AC sensing signal f_s .

$$C = \frac{1}{2\pi f_s X_c} \quad (3)$$

Supporting Information

Supporting Information is available from the Wiley Online Library or from the author.

Acknowledgements

Z.Y., D.M., I.S., and C.K. acknowledge funding by the Max Planck Society, Germany. D.M. acknowledges funding by the Max Planck ETH Center for Learning Systems. Z.Y., G.K., I.S., E.A., and C.K. acknowledge funding from The David and Lucile Packard Foundation and startup funds from the University of Colorado, Boulder. The authors thank the International Max Planck Research School for Intelligent Systems (IMPRS-IS) for supporting Z.Y. and I.S. The authors thank the team in the central scientific facility for robotics of the Max Planck Institute for Intelligent Systems for helping to design the integrated high-voltage driving electronics and Sophie Kirkman for help with proofreading the manuscript.

Open access funding enabled and organized by Projekt DEAL.

Conflict of Interest

E.A. and C.K. are co-founders of Artimus Robotics Inc., a company focused on commercializing HASEL actuators. E.A. and C.K. are inventors on US patent number 10995779, US Application No. 17/198909, US Application No. 16/978292, European Application EP18770604.9A, and European Application EP3762618A4, which cover fundamentals and basic designs of HASEL actuators.

Data Availability Statement

The data that support the findings of this study are openly available in KEEPER at <https://keeper.mpdl.mpg.de/d/ed19b91575ea4e12b202/>, reference number 393.

Keywords

artificial muscles, capacitive sensing, electrostatic actuators, grippers, soft robotics

Received: August 6, 2022

Revised: October 20, 2022

Published online: November 11, 2022

- [1] G. J. Monkman, S. Hesse, R. Steinmann, H. Schunk, *Robot grippers*, Wiley-VCH, Hoboken, NJ, USA **2007**.
- [2] a) A. Bicchi, *IEEE Trans. Robot.* **2000**, *16*, 652; b) K. Tai, A.-R. El-Sayed, M. Shahriari, M. Biglarbegian, S. Mahmud, *Robot.* **2016**, *5*, 11.
- [3] a) S. Kim, C. Laschi, B. Trimmer, *Trends Biotechnol.* **2013**, *31*, 287; b) D. Rus, M. T. Tolley, *Nature* **2015**, *521*, 467; c) C. Laschi, B. Mazzolai, M. Cianchetti, *Sci Robot* **2016**, *1*, eaah3690; d) P. Polygerinos, N. Correll, S. A. Morin, B. Mosadegh, C. D. Onal, K. Petersen, M. Cianchetti, M. T. Tolley, R. F. Shepherd, *Adv. Eng. Mater.* **2017**, *19*, 1700016; e) G. M. Whitesides, *Angew. Chem., Int. Ed.* **2018**, *57*, 4258; f) P. Rothmund, Y. Kim, R. H. Heisser, X. Zhao, R. F. Shepherd, C. Keplinger, *Nat. Mater.* **2021**, *20*, 1582; g) N. El-Atab, R. B. Mishra, F. Al-Modaf, L. Joharji, A. A. Alsharif, H. Alamoudi, M. Diaz, N. Qaiser, M. M. Hussain, *Adv. Intell. Syst.* **2020**, *2*, 2000128.
- [4] S. Hirose, Y. Umetani, *Mech. Mach. Theory* **1978**, *13*, 351.
- [5] a) O. A. Araromi, I. Gavrilovich, J. Shintake, S. Rosset, M. Richard, V. Gass, H. R. Shea, *IEEE ASME Trans. Mechatron.* **2015**, *20*, 438; b) E. Brown, N. Rodenberg, J. Amend, A. Mozeika, E. Steltz, M. R. Zakin, H. Lipson, H. M. Jaeger, *Proc. Natl. Acad. Sci. USA*

- 2010, 107, 18809; c) K. C. Galloway, K. P. Becker, B. Phillips, J. Kirby, S. Licht, D. Tchernov, R. J. Wood, D. F. Gruber, *Soft Robot* **2016**, 3, 23; d) P. Glick, S. A. Suresh, D. Ruffatto, M. Cutkosky, M. T. Tolley, A. Parness, *IEEE Robot. Autom. Lett.* **2018**, 3, 903; e) F. Ilievski, A. D. Mazzeo, R. F. Shepherd, X. Chen, G. M. Whitesides, *Angew. Chem., Int. Ed.* **2011**, 50, 1890; f) M. Manti, T. Hassan, G. Passetti, N. D'Elia, C. Laschi, M. Cianchetti, *Soft Robot* **2015**, 2, 107; g) B. Mosadegh, P. Polygerinos, C. Keplinger, S. Wennstedt, R. F. Shepherd, U. Gupta, J. Shim, K. Bertoldi, C. J. Walsh, G. M. Whitesides, *Adv. Funct. Mater.* **2014**, 24, 2163; h) S. Shian, K. Bertoldi, D. R. Clarke, *Adv. Mater.* **2015**, 27, 6814; i) J. Shintake, S. Rosset, B. Schubert, D. Floreano, H. Shea, *Adv. Mater.* **2016**, 28, 231; j) W. Wang, S.-H. Ahn, *Soft Robot* **2017**, 4, 379; k) S. Wang, H. Luo, C. Linghu, J. Song, *Adv. Funct. Mater.* **2021**, 31, 2009217; l) X. Tang, K. Li, Y. Liu, D. Zhou, J. Zhao, *Smart Mater. Struct.* **2019**, 28, 035019.
- [6] J. Shintake, V. Cacucciolo, D. Floreano, H. Shea, *Adv. Mater.* **2018**, 30, 1707035.
- [7] S. Zaidi, M. Maselli, C. Laschi, M. Cianchetti, *Curr Robot Rep* **2021**, 2, 355.
- [8] a) Y. Hao, Z. Gong, Z. Xie, S. Guan, X. Yang, Z. Ren, T. Wang, L. Wen, presented at 2016 35th Chinese Control Conference (CCC), Chengdu, China, July **2016**; b) R. Deimel, O. Brock, *Int. J. Robot. Res.* **2016**, 35, 161; c) S. Terryn, J. Brancart, D. Lefeber, G. Van Assche, B. Vanderborght, *Sci Robot* **2017**, 2, eaan4268.
- [9] J. Hughes, U. Culha, F. Giardina, F. Guenther, A. Rosendo, F. Iida, *Front Robot AI* **2016**, 3, 69.
- [10] a) M. T. Tolley, R. F. Shepherd, B. Mosadegh, K. C. Galloway, M. Wehner, M. Karpelson, R. J. Wood, G. M. Whitesides, *Soft Robot* **2014**, 1, 213; b) S. M. Mirvakili, D. Sim, I. W. Hunter, R. Langer, *Sci Robot* **2020**, 5, eaaz4239.
- [11] a) N. Farrow, N. Correll, *IEEE/RSJ International Conference on Intelligent Robots and Systems (IROS)* **2015**, 2015, 2317; b) B. S. Homberg, R. K. Katzschmann, M. R. Dogar, D. Rus, *International Conference on Intelligent Robots and Systems (IROS)* **2015**, 2015, 1698; c) T. G. Thuruthel, B. Shih, C. Laschi, M. T. Tolley, *Sci Robot* **2019**, 4, eaav1488.
- [12] a) E. Acome, S. K. Mitchell, T. G. Morrissey, M. B. Emmett, C. Benjamin, M. King, M. Radakovitz, C. Keplinger, *Science* **2018**, 359, 61; b) N. Kellaris, V. G. Venkata, G. M. Smith, S. K. Mitchell, C. Keplinger, *Sci Robot* **2018**, 3, 3276; c) S. K. Mitchell, X. Wang, E. Acome, T. Martin, K. Ly, N. Kellaris, V. G. Venkata, C. Keplinger, *Adv. Sci.* **2019**, 6, 1900178; d) P. Rothemund, N. Kellaris, S. K. Mitchell, E. Acome, C. Keplinger, *Adv. Mater.* **2021**, 33, 2003375; e) X. Wang, S. K. Mitchell, E. H. Rumley, P. Rothemund, C. Keplinger, *Adv. Funct. Mater.* **2020**, 30, 1908821.
- [13] a) N. Kellaris, P. Rothemund, Y. Zeng, S. K. Mitchell, G. M. Smith, K. Jayaram, C. Keplinger, *Adv. Sci.* **2021**, 8, 2100916; b) D. Tscholl, S.-D. Gravert, A. X. Appius, R. K. Katzschmann, *Robotics* **2022**; c) T. Park, K. Kim, S.-R. Oh, Y. Cha, *Soft Robot* **2020**, 7, 68; d) Z. Yoder, N. Kellaris, C. Chase-Markopoulou, D. Ricken, S. K. Mitchell, M. B. Emmett, R. F. Weir, J. Segil, C. Keplinger, *Front Robot AI* **2020**, 7, 586216.
- [14] a) S. K. Mitchell, T. Martin, C. Keplinger, *Adv. Mater. Technol.* **2022**, 7, 2101469; b) S. Schlatter, P. Illenberger, S. Rosset, *HardwareX* **2018**, 4, e00039.
- [15] K. Ly, N. Kellaris, D. McMorris, B. K. Johnson, E. Acome, V. Sundaram, M. Naris, J. S. Humbert, M. E. Rentschler, C. Keplinger, N. Correll, *Soft Robot* **2020**, 8, 673.
- [16] a) S. Rosset, B. M. O'Brien, T. Gisby, D. Xu, H. R. Shea, I. A. Anderson, *Smart Mater. Struct.* **2013**, 22, 104018; b) T. A. Gisby, B. M. O'Brien, I. A. Anderson, *Appl. Phys. Lett.* **2013**, 102, 193703; c) C. Keplinger, M. Kaltenbrunner, N. Arnold, S. Bauer, *Appl. Phys. Lett.* **2008**, 92, 192903.
- [17] P. Rothemund, S. Kirkman, C. Keplinger, *Proc Natl Acad Sci USA* **2020**, 117, 16207.
- [18] N. Kellaris, V. G. Venkata, P. Rothemund, C. Keplinger, *Extreme Mech Lett.* **2019**, 29, 100449.
- [19] S. Coyle, C. Majidi, P. LeDuc, K. J. Hsia, *Extreme Mech. Lett.* **2018**, 22, 51.
- [20] R. Maccurdy, R. Katzschmann, K. Youbin, D. Rus, *IEEE International Conference on Robotics and Automation (ICRA)* **2016**, 3878.
- [21] A. Tairyck, I. Anderson, Distributed sensing: multiple capacitive stretch sensors on a single channel, SPIE, Bellingham, WA **2017**, 10163.
- [22] S. Pourazadi, A. Shagerdmootaab, H. Chan, M. Moallem, C. Menon, *Smart Mater. Struct.* **2017**, 26, 115007.